Supplementary Methods

IgG preparation and injections

IgG was prepared from the plasma of anti-MuSK-positive myasthenia gravis patients and human control plasma as previously detailed (Cole et al., 2008). Concentrations of IgG were determined by nephelometry. Patient numbers are the same as in our previous papers (AM1, 2, 3 and 4) with the addition of a new patient (AM5). The batches used are listed in Supplementary Table S1. For example, AM4.2 refers to IgG batch number 2 from anti-MuSK-positive patient number 4. This is the same patient 4 as described in (Cole et al., 2010). Batches AM 4.2, 4.4 and 4.5 were all prepared from plasma exchange filtrates collected from patient 4 but on different days when the patient's disease severity and anti-MuSK titres differed. Control IgG was from pooled plasma from therapeutic venesection of hemochromatosis patients screened negative for both anti-AChR and anti-MuSK.

In addition to the daily injections of IgG, mice received a single i.p. injection of cyclophosphamide monohydrate (300mg/kg; Sigma, St Louis MO, USA; 10mg/ml in sterile 0.9% NaCl) 24hr after the first IgG injection to suppress any potential active immune response to the human proteins (Otterness and Chang, 1976; Toyka et al., 1975).

Immunostaining and morphometric analysis

Upon snap freezing the tibialis anterior (TA) and the diaphragm muscles were sectioned longitudinally to the long axis of the muscle fibres. Sections (20 μm) were fixed for 15 minutes in 2% paraformaldehyde/PBS at room temperature, immersed in

PBS containing 0.1M glycine for 30 minutes, permeabilised in methanol (-20°C) for 7mins and blocked for 1hr in PBS containing 0.2% Triton and 2% BSA. Slides were washed with PBS three times between every step. Sections were immunoreacted with rabbit anti-synaptophysin (1:200; Dako Australia, Sydney) overnight at 4°C followed by fluoresceine isothiocyanate (FITC)-conjugated donkey anti-rabbit IgG (Jackson ImmunoResearch). AChRs were stained with α-bungarotoxin (Alexa 555-BGT, 1:200). Z-stacks of NMJs were collected by confocal scanning laser microscopy (Zeiss LSM510Meta confocal microscope) as described (Gervásio and Phillips, 2005). ImageJ was used to produce Z-projections of the stacks (extended-focus images). Metamorph software (Molecular Devices, Inc., CA, USA) was used to split the colour channels and an intensity threshold was set to isolate the region of interest (AChR clusters or nerve terminal) from background. Metamorph's integrated morphometry analysis tool was used to measure the area and intensity of the postsynaptic AChR cluster and presynaptic nerve terminal staining. The area of overlap (pixel by pixel) was determined using the co-localisation plug-in of the Metamorph program.

For the analysis of transverse sections, maximum intensity projection images (~12 x 1μm spacing) were sampled as above and images were coded by M.M. AChR staining patterns in the images were classified blindly by N.G. into the categories described in the text. Double labelling for AChR and AChE was carried out as described above except that AChE was labelled with Alexa 647-fasciculin 2 (Krejci et al., 2006) diluted 1:200 in 2% BSA/PBS for 1hr at room temperature.

Supplementary Table S1

Batches of human IgG used in this study*

Anti-MuSK Patient No. ψ	**IgG Batch**	**Amount injected** (mg/day)	**MG severity at time of plasma collection ***	**Weakness grade in mice (mean)** †
5	AM5	20	MGFA 4B (severe)	Grade 2.0
4	AM4.4	45	MGFA 4B (severe)	Grade 1.6
4	AM4.5	35	MGFA 3B (moderate)	Grade 1.3
4	AM4.5	25	MGFA 3B (moderate)	Grade 0
4	AM4.2	45	MGFA 2B (mild)	Grade 0
Control	pooled	45	-	Grade 0

ψ Patient numbering system is as per our previous publications. Control IgG was pooled from patients on therapeutic venesection for hemochromatosis and was screened negative for anti-MuSK and anti-AChR.

* MGFA: Myasthenia Gravis Foundation of America score

† Average weakness grade produced in mice at the end of the IgG injection series (14-15 days) according to the grading scheme of Stacy et al (Stacy et al., 2002) and as described in the text.

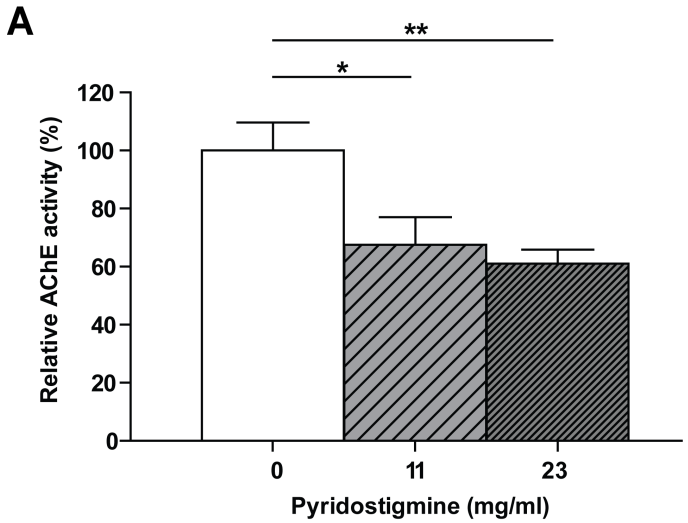

Supplementary Figure S1. Inhibition of blood cholinesterase activity in mice with a subcutaneous minipump delivering pyridostigmine.

An osmotic minipump filled with the indicated concentration of pyridostigmine bromide or mestinon buffer (vehicle) was implanted subcutaneously. Whole blood AChE activity was calculated after mice were sacrificed, largely as described by (Haigh et al., 2008). Blood (50-300µl) was drawn from the heart at sacrifice and was snap frozen in liquid nitrogen. A small aliquot of thawed blood (typically 1µl diluted in 39µl distilled water), was mixed with 50mM sodium phosphate buffer (pH 8.0), 0.2mM of the chromophore 4,4'-dithiopyridine (DTP) and 1mM acetylthiocholine iodide in a microtitre well to a final volume of 60µl. Assays were performed with 3-4 replicates. A 6-min kinetic assay was performed at 25ºC (7-9sec intervals between readings) recording absorbance at 324nm with a microplate spectrophotometer (FLUOstar Omega, BMG Labtech Australia). Kinetic assay values were normalised to absorbance values for the samples at 415 and 445nm. The normalised data was analysed via Graphpad Prism (GraphPad Software, CA, USA) and Excel spreadsheets by comparing each data set's curve fit between a nonlinear regression of a straight

line (first order polynominal) and the fit of a second model (second order polynominal) (Cleland, 1967). The activity of AChE (%) relative to naive mice was calculated from the slopes for the first order polynominal (straight line) for each data set. The highest dose of pyridostigmine in our pilot experiments (47mg/ml in Alzet pump model 1007D) caused oral and nasal secretions, muscle fasciculation and breathing difficulties in the first 24hr, consistent with acetylcholinesterase intoxication described before (Hudson et al., 1986). Similar side effects were also found by Engel et al. in a long term study of neostigmine in rats (Engel et al., 1973). These mice were killed for ethical reasons. Lower doses of pyridostigmine (11 or 23mg/ml) caused 32 ± 9% and 39 ± 4% reductions in blood cholinesterase respectively, but without signs of intoxication such as oral or ocular secretions or increased sensitivity to sounds (startle response to a hand clap). The 23mg/ml dose was chosen as achieving a level of AChE inhibition comparable to that found in effectively treated MG patients of 45-60% (Henze et al., 1991). Bars show the mean ± SEM for n=3 mice (*$P < 0.05$; **$P < 0.01$ one-way ANOVA Bonferroni's multiple comparison post-test).

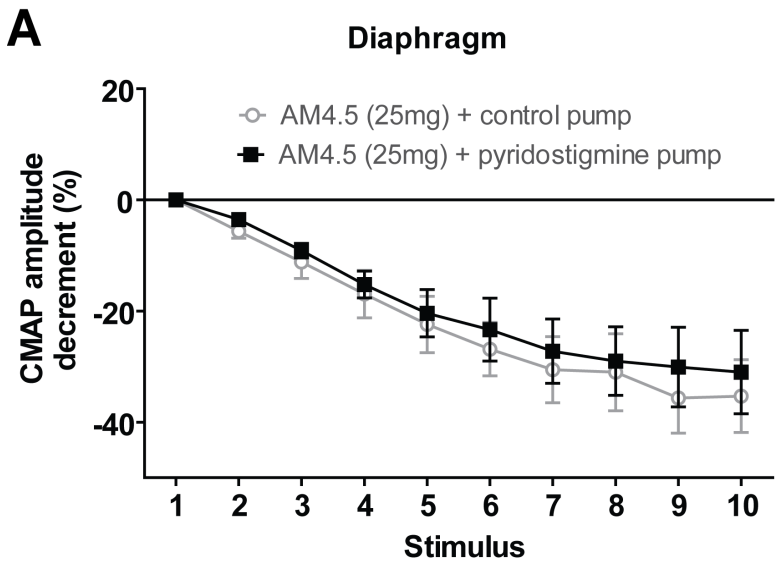

Supplementary Figure S2. Decremental responses of CMAP upon repetitive nerve stimulation.

Mice received daily injections of AM4.5 IgG (25mg/day) for 17 days and were treated for the last 9 days with pyridostigmine (23mg/ml; filled black squares) or with vehicle (open gray circles). Recordings of CMAPs during repetitive stimulation of the nerve (3 per sec) were made from the surface of the isolated hemidiaphragm *ex-vivo*. Endplates showed a similar decremental response in mice treated with either pyridostigmine or vehicle. It seems likely that the pyridostigmine had been washed out of the very thin isolated hemidiaphragm preparation before the recordings were made (the muscle was placed in pyridostigmine-free ringer solution for 30-60 minutes before recordings). Data represent the mean ± SEM for three runs in each diaphragm of 3 mice in each treatment group.

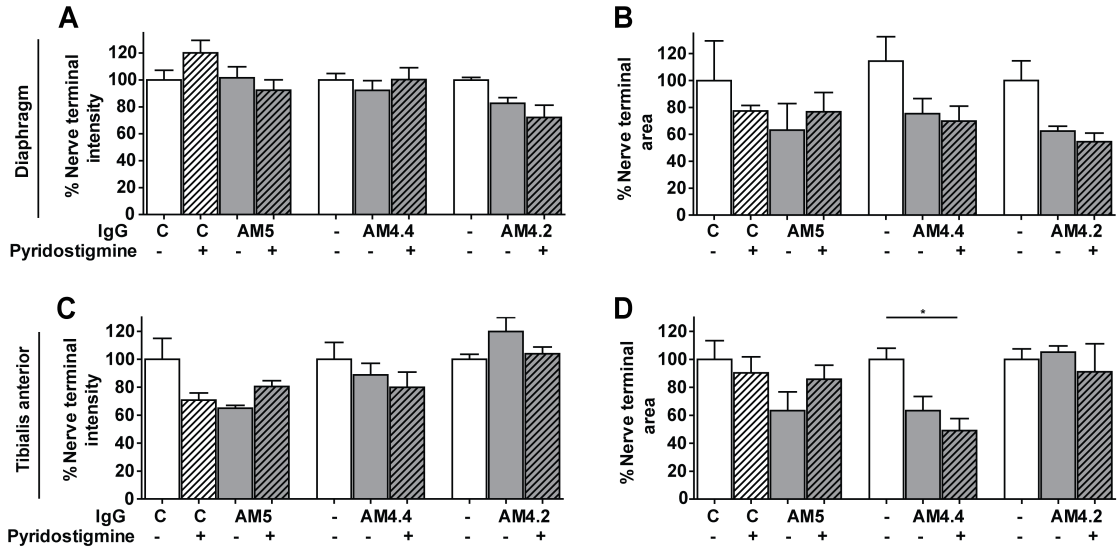

Supplementary Figure S3. Modest effects of anti-MuSK IgG and pyridostigmine on the presynaptic nerve terminal.

The effects of anti-MuSK IgGs and pyridostigmine upon the staining intensity and area of presynaptic nerve terminals are shown for the diaphragm (**A&B**) and TA muscles (**C&D**). Bars compare the area (**B&D**) and staining intensity (**A&C**) of synaptophysin immunoreactivity at endplates in mice injected with anti-MuSK IgG, with or without pyridostigmine treatment, relative to control animals (naive mice or mice injected with control IgG for 14 days). A pump containing pyridostigmine or vehicle was implanted on days 7 or 8, as described in Figure 1. Data were normalised to values for mice injected with control IgG (C) and naive controls. Data represent means values for n=3-5 mice (21-62 endplates per mouse; *$P < 0.05$ one-way ANOVA with Bonferroni's multiple comparison post-test).

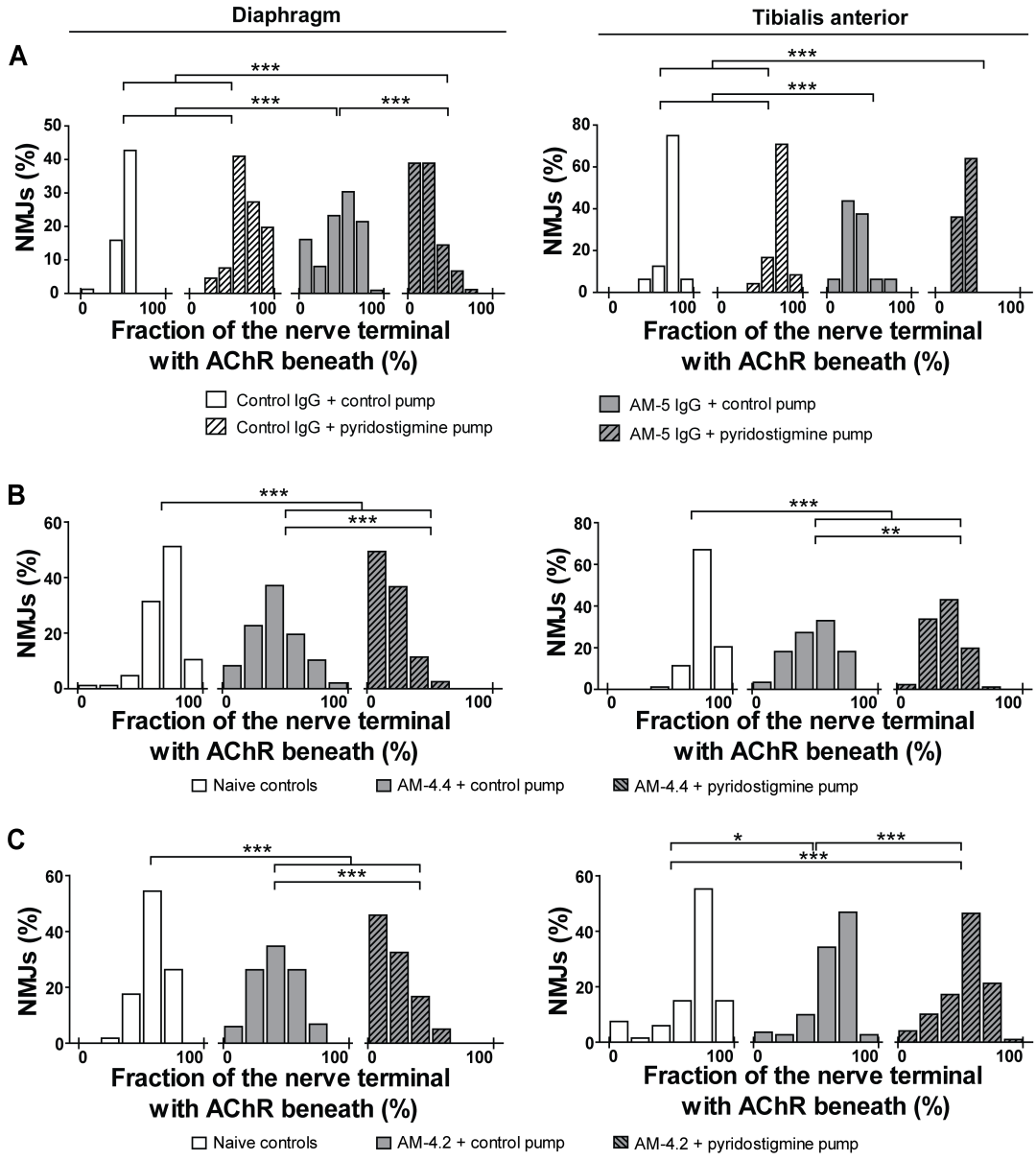

Supplementary Figure S4. Percentage of the nerve terminal with AChRs aligned beneath it.

Frequency histograms represent the percentage of each nerve terminal that was aligned with densely packed postsynaptic AChRs on days 14-15 of the IgG injection series. Treatment (pyridostigmine or vehicle) was delivered for the last 7 days of the injection series. Treatment group keys are shown immediately beneath each set of histograms. (**A**) Mice injected with control human IgG or anti-MuSK IgG AM5, with

or without pyridostigmine treatment (treatment groups as shown in Fig. 1A). (**B**) Effect of AM4.4 with or without pyridostigmine treatment. (**C**) Effect of anti-MuSK IgG AM4.2 with or without pyridostigmine treatment. Endplate data in each distribution represents a total of 60-122 endplates pooled from 3 mice (*P < 0.05; **P < 0.01; ***P < 0.001 Kruskal-Wallis with Dunn's multiple comparison post-test). Note that injection of anti-MuSK IgG alone produced significant shifts towards nerve terminals with reduced areas of AChR aligned beneath them. This shift was augmented by pyridostigmine treatment, particularly in the diaphragm muscle.

References

Cleland WW. Enzyme kinetics. Annu Rev Biochem 1967; 36: 77-112.

Cole RN, Ghazanfari N, Ngo ST, Gervasio OL, Reddel SW, Phillips WD. Patient autoantibodies deplete postsynaptic Muscle Specific Kinase leading to disassembly of the ACh receptor scaffold and myasthenia gravis in mice. J Physiol (Lond) 2010; 588.17: 3217-3229.

Cole RN, Reddel SW, Gervásio OL, Phillips WD. Anti-MuSK patient antibodies disrupt the mouse neuromuscular junction. Ann Neurol 2008; 63: 782-789.

Engel AG, Lambert EH, Santa T. Study of long-term anticholinesterase therapy. Neurology 1973; 23: 1273-1281.

Gervásio OL, Phillips WD. Increased ratio of rapsyn to ACh receptor stabilizes postsynaptic receptors at the mouse neuromuscular synapse. J Physiol 2005; 562.3: 673-685.

Haigh JR, Lefkowitz LJ, Capacio BR, Doctor BP, Gordon RK. Advantages of the WRAIR whole blood cholinesterase assay: Comparative analysis to the micro-

Ellman, Test-mate ChE™, and Michel (ΔpH) assays. Chemico-Biological Interactions 2008; 175: 417-420.

Henze T, Nenner M, Michaelis HC. Determination of erythrocyte-bound acetylcholinesterase activity for monitoring pyridostigmine therapy in myasthenia gravis. J Neurol 1991; 238: 225-229.

Hudson CS, Foster RE, Kahng MW. Ultrastructural effects of pyridostigmine on neuromuscular junctions in rat diaphragm. Neurotoxicol 1986; 7: 167-186.

Krejci E, Valenzuela IM-P, Ameziane R, Akaaboune M. Acetylcholinesterase dynamics at the neuromuscular junction of live animals. J Biol Chem 2006; 281: 10347-10354.

Otterness IG, Chang Y-H. Comparative study of cyclophosphamide, 6-mercaptopurine, azathiopurine and methotrexate. Relative effects on the humoral and the cellular immune response in the mouse. Clin Exp Immunol 1976; 26: 346-354.

Stacy S, Gelb BE, Koop BA, Windle JJ, Wall KA, Krolick KA, et al. Split tolerance in a novel transgenic model of autoimmune myasthenia gravis. J Immunol 2002; 169: 6570-6579.

Toyka KV, Brachman DB, Pestronk A, Kao I. Myasthenia gravis: passive transfer from man to mouse. Science 1975; 190: 397-399.